Conventional and unconventional Turing patterns

Cite as: J. Chem. Phys. **96**, 664 (1992); https://doi.org/10.1063/1.462450
Submitted: 18 July 1991 • Accepted: 26 September 1991 • Published Online: 04 June 1998

V. Dufiet and J. Boissonade

Conventional and unconventional Turing patterns

V. Dufiet and J. Boissonade
Centre de Recherche Paul Pascal, Université Bordeaux I, Avenue Schweitzer, F-33600 Pessac, France

(Received 18 July 1991; accepted 26 September 1991)

The formation of two-dimensional Turing patterns in nonequilibrium chemical systems is studied by numerical simulations with an activator-substrate depletion model. The relative stabilities of the different hexagonal patterns and the striped patterns are discussed, in particular in the vicinity of the transition, and compared with the present state theory. The generic instabilities of the striped patterns are evidenced. In particular, we report the formation of stable zigzag patterns which share features both of one-dimensional and two-dimensional patterns. We also provide examples of temporal evolution in a weakly confined system.

I. INTRODUCTION

In this paper, we shall be concerned with monophasic isothermal chemical systems kept far from equilibrium by a permanent supply of fresh reactants. The term "monophasic" rules out heterogeneous systems, surface reactions, and reactions involving precipitates. The transport processes are supposed to be limited to molecular diffusion, excluding convection effects. In these conditions the concentrations of the different species evolve in space and time according to a system of reaction–diffusion equations. Most systems asymptotically approach a stationary state which preserves the symmetries imposed by the feeding process. For the sake of simplicity, this state will be called "uniform" in the following, by reference to the special case of a uniform feed. The latter assumption is commonly used in theoretical work. If appropriate kinetics, such as autocatalysis and substrate inhibition mechanisms, are involved, the uniform state can become unstable when a control parameter crosses a critical value and various structures can spontaneously develop.[1–5] If, at the bifurcation point, the first unstable mode corresponds to a nonzero critical wave number $k = k_c$, a spatial pattern of wavelength $\lambda = 2\pi/k_c$ forms just above the transition point. When the pattern resulting from this symmetry breaking instability is stationary, it is called a "Turing structure." The emergence of such structures has been predicted almost forty years ago[6] and thoroughly studied from a theoretical point of view, in particular in relation with their possible role in biological morphogenesis.[4,7–9] In addition to special kinetics, another necessary condition for a Turing instability to occur is that the diffusion coefficients of at least two species be different. From a practical point of view, these are stringent conditions; they have precluded the production of these patterns in the laboratory until recently, when a stationary concentration pattern, with the expected characters, was obtained by Castets *et al.*,[10–12] who studied the chlorite–iodide–malonic acid reaction in a film of inert gel. The observed pattern, localized in a narrow band orthogonal to the gradient induced by the feed, is made of stripes or hexagons. The distribution of concentrations in the direction of the observation, i.e., in the depth of the film, which is significantly larger than the wavelength (~ 0.2 mm), is still presently under investigation. Recently, these experiments have been repeated by Ouyang and Swinney, with a different reactor geometry.[13] In the latter, the system is a thin film, uniformly fed through two large opposite circular areas; the direction of observation is the direction of the gradient induced by the feed, orthogonal to these circular areas. According to the temperature, the systems exhibit stripes or hexagonal symmetry on extended domains and the transition from the uniform state to hexagonal structures was quantitatively studied. The authors do not report any evidence of self-organization in the film depth, so that the pattern can be considered as two dimensional. A simplified but realistic model has been proposed by Lengyel and Epstein to account for the Turing instability for this specific reaction;[14] in particular, the model provides an explanation for the effective difference between diffusion coefficients.

In regard to these important developments, it becomes useful to revisit the previous work on nonlinear patterning phenomena associated with the formation of Turing structures in two-dimensional systems. This problem has been addressed in the field of biological growth processes,[4] but a general nonlinear pattern selection theory has also been developed, mainly in relation with hydrodynamics. The state of the art, in this particular context, is well reviewed in Ref. 15. The formalism is based on the reduction to lowest orders of the reaction–diffusion equations to a set of ordinary differential equations for the temporal evolution of the amplitudes of the different unstable modes. The multiplicity of these modes results both from the degeneracy associated with rotational invariance in isotropic systems—only the modulus $|\mathbf{k}_c|$ is defined, not the orientation—and of the increasing finite bandwidth of permitted modes, when the distance to criticality increases. Selection of particular structures occurs both at the linear stage—the most unstable modes growing faster than the others—and at the nonlinear stage. The mutual nonlinear coupling of modes determines their saturation, imposes relations between wave vectors, and initiates secondary instabilities. Only a few papers apply this approach, on which we shall focus here, to chemical systems.[16–23] Unfortunately, a full derivation of amplitude equations from the original reaction–diffusion system is an extremely tedious procedure which has only been achieved in a small number of cases,[16,18,20,22,23] often with additional

 0021-9606/92/010664-10$06.00

simplifications or with particular symmetries. The form of the equations is more commonly derived from the symmetries of the anticipated structures, giving priority to the universal properties. Thus, it is highly suitable to test their relevance to chemical patterns by solving the original system of reaction–diffusion equations.

Here, we report a great number of numerical experiments on a particular two-dimensional model. In a finite system the spectrum of modes fitting the boundary conditions is discrete. The size of the studied systems was chosen large enough to minimize the effects of this quantification, and—except for a few experiments reported in Sec. IV—small enough to be spatially coherent and free of structural defects. We successively exhibit the expected conventional Turing patterns, i.e., hexagons and stripes, and perform a quantitative study of the bifurcations from the uniform to the patterned state. This study was initially motivated by the results of Ref. 13. Then, we shall report the numerical study of generic secondary instabilities. Finally, we show that the so-called zigzag instability can be saturated to provide an unconventional stable striped pattern.

II. MODEL AND METHODS

A. The model

Since we are interested in universal generic patterning properties, we have preferred, for our purpose, a general robust model to a more realistic one, like the scheme of Ref. 14, which is more suited to the discussion of a specific reaction. We have retained the Schnackenberg model,[24] a simplified variant of the well-known "Brussellator".[25] This two-variable scheme has several major advantadges: (a) The Turing space, i.e., the domain of control parameters where the model exhibits a Turing instability, is large and robust, which is difficult to meet with a realistic model. (b) Like for the "Brussellator," many properties have been previously calculated analytically, in particular by Murray.[4,26] (c) When performed in similar geometrical conditions, our previous numerical simulations[12] emulate well the qualitative behavior observed in the original experiments.[10,11] This model has been found especially convenient for this purpose, since the dynamics of the input species are independent of the intermediate species concentrations. Here, the computations should be more relevant to the experiments of Ref. 13.

The reaction steps of the Schnackenberg model are

$$A \xrightarrow{k_1} X,$$

$$X \xrightarrow{k_2} \text{products},$$

$$2X + Y \xrightarrow{k_3} 3X,$$

$$B \xrightarrow{k_4} Y,$$

where A and B are the pool species that will be assumed to be uniform and X and Y are the intermediate species. In the "Brussellator," the last step is replaced by $B + X \rightarrow Y$. This scheme belongs to the class of the so-called "activator-substrate depleted" models:[7,27] when a pattern emerges, the concentrations of X and Y are out of phase by π. Using the same character for the species and their concentration, we define the following dimensionless variables:

$$t^* = \frac{D_X t}{L^2},\ \mathbf{r}^* = \frac{\mathbf{r}}{L},\ d = \frac{D_Y}{D_X},\ \gamma = L^2 k_2 / D_X,$$

$$a = \frac{k_1}{k_2}\left(\frac{k_3}{k_2}\right)^{1/2} A,\ b = \frac{k_4}{k_2}\left(\frac{k_3}{k_2}\right)^{1/2} B,$$

$$u = \left(\frac{k_3}{k_2}\right)^{1/2} X,\ v = \left(\frac{k_3}{k_2}\right)^{1/2} Y.$$

It is suitable to choose the typical length scale L of the same order as the size of the system, but not necessarily this size itself. Alternative scalings, based on natural diffusion time scales and lengths would be possible. Nevertheless, we have retained this specific form to conform with the previous analytical results of the literature.[4] This form is actually convenient when the length scale change in time, e.g., when discussing embryogenesis phenomena.

From the mass action law, and with the above scaling, the reaction–diffusion equations can be reduced to the following standard form:[4,12]

$$\frac{\partial u}{\partial t} = \gamma(a - u + u^2 v) + \Delta_r u, \tag{1}$$

$$\frac{\partial u}{\partial t} = \gamma(b - u^2 v) + d\Delta_r v, \tag{2}$$

where the asterisks were dropped for convenience and Δ_r is the Laplacian operator. To sum up, the scaled quantities a, b, u, v are respectively proportional to the concentrations of A, B, X, Y, the constant γ is the scaled global reaction rate and d is the ratio of the diffusion coefficient of the activator X to the diffusion coefficient of the substrate Y. In all subsequent computations, we shall use the values $\gamma = 10\,000$, $d = 20$, and a system size of order unity.

From linear stability analysis one can show that, when $d > 1$, a Turing pattern forms in the parameter region where the following conditions are simultaneously fulfilled:[4,26]

$$0 < b - a < (a + b)^3,\ d(b - a) > (a + b)^3,$$

$$[d(b - a) - (a + b)^3]^2 > 4d(a + b)^4. \tag{3}$$

The limits of this Turing space as a function of a and b are drawn on Fig. 1 when $d = 20$. In order to avoid spurious effects in the vicinity of unstationary regions, we shall focus on the transition located on the right side of the diagram.

B. Boundary and initial conditions

All computations were performed with periodic boundary conditions in a square box, except for a few studies of regular hexagonal structures where a slight adjustment on one side was made necessary to satisfy simultaneously hexagonal symmetry and boundary periodicity. The system size ranges from $L = 1$ to $L = 2.56$ ($L = 4$ for the studies of the Eckhaus instability) for a typical wavelength $\lambda \sim 0.1$. The system size was chosen in accordance with the nature of the problem in order to minimize the effects of mode quantification. The largest sizes were mainly used to test the behavior

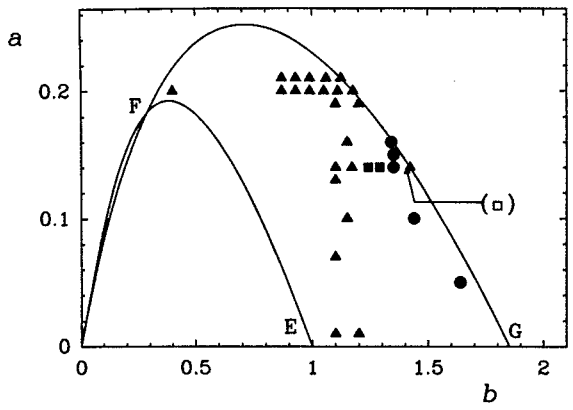

FIG. 1. Turing space. Path EFGE encloses the Turing patterns domain in the (a,b) parameter space. Nature and stability of computed patterns (△: stable hexagons H1; ▲: stable hexagons H2; ●: stable stripes; □: hexagons H1 and stripes are both stable; ■: hexagons H2 and stripes are both stable).

of weakly confined systems. Actual sizes are given in the corresponding figure captions.

The choice of initial conditions is consistent with the nature—generic or specific—of the tested instabilities. A spatial perturbation is added to a basic state. The basic state was either a uniform state, in general the unstable steady state, or a structured state (striped or hexagonal symmetry) obtained from former computations or by superposition of elementary sinusoidal modes. In some studies of the stability of the striped patterns, the basic pattern was previously obtained, when possible, in a one-dimensional computation. Three types of perturbation were used: (a) random noise, all points of space being uncorrelated, (b) superposition of a set of different sinusoidal modes with random phases and random noise added. This process introduces long wavelength modes in the noise, (c) small amplitude patterns resulting from a superposition of sinusoidal modes, similar to a basic state. This allows, in particular, for checking the stability of a structure against another one.

C. Numerical techniques

All numerical experiments were performed by finite difference methods with spatial stepsize $\Delta x = 0.01$. The few 1D computations were carried out by the method of lines with a fourth order, semi-implicit, variable time step Rosenbrock integrator.[28] The integration of two-dimensional systems was achieved with an odd–even implicit hopscotch method,[29–31] modified to account for the nonlinear terms. The stepsize was generally fixed to $\Delta t = 5.10^{-6}$, to be compared with the typical reaction time $\gamma^{-1} = 10^{-4}$. An explicit Euler method is used during the first steps, with $\Delta t = 4.10^{-7}$ to relax random noise.

D. Display of results

Most of our results are displayed as images of the stationary patterns, obtained asymptotically. We always represent concentration u; the corresponding patterns of v are similar with inversion of density. The concentrations are represented on laser prints with 32 grey scale levels, using full scale between the absolute minimum (black) and the absolute maximum (white). Thus, the density correspond to relative variations, not to absolute concentrations.

III. CONVENTIONAL PATTERNS: HEXAGONS VERSUS STRIPES

A. Nature of patterns

The basic patterns that tesselate the plane are, respectively, parallel stripes (frequently referred as "rolls" in hydrodynamics), patterns with hexagonal symmetry (triangles, hexagons), and rhombs. Hexagonal and striped patterns were observed in early work on models relevant to biological systems.[16,32]

Several authors have discussed the respective stabilities of these patterns on the basis of amplitude equations.[20,23,33–35] Let us summarize the results of the theory, as gathered in Ref. 34. Hexagons should appear first via a subcritical bifurcation, while stripes arise supercritically but are unstable, becoming stable only at larger values of the control parameter. Hexagons become unstable at still higher values; there is a region of bistability where both patterns are stable. Stable rhombs can form in place of stripes for smaller values of the—angular dependent—cubic term in the amplitude equations. Like stripes, they first arise as unstable patterns via a supercritical bifurcation. Some symmetries set the quadratic term to zero;[15,23,33–35] then, only stripes are stable and arise via a pitchfork-type bifurcation, but, except for very peculiar models,[23] regular chemical systems have a quadratic term and hexagonal patterns should always bifurcate first. The theory has been extended to three-dimensional systems by Walgraef *et al.*[18,20–22] The patterns appear successively through subcritical bifurcations with decreasing dimensionality—body centered cubic (3D), hexagonal prisms (2D)—, while the last structure—parallel planes (1D)—arises supercritically. The stability properties are a straightforward extension of the two-dimensional case. Recent simulations by De Wit *et al.* with the Brussellator model support these calculations.[22] Although not enough emphasized, for a given wavelength, there are two different branches with hexagonal symmetry, corresponding to a phase shift of π. Both are unstable in the vicinity of the bifurcation point. On the first one, referred further as H1, the maxima of u (in white) form a honeycomb lattice, the minima (in black) form a triangular lattice. On the second branch, referred as H2, the maxima of u form a triangular lattice, the minima form a honeycomb lattice. The reverse situation holds for v.

We have observed striped and hexagonal patterns, starting from a uniform state with random noise added (Fig. 2). The nature of the patterns obtained in a series of experiments is indicated in the diagram in Fig. 1. At large values of a, hexagonal symmetry of type H2 prevails; at small values of a, the system exhibits predominantly stripes but a few hexagonal structures of type H1 are observed in the vicinity of the bifurcation. We have also observed regions where both types of structures are stable, which defines a bistability range, but, when a increases, the change between the two main do-

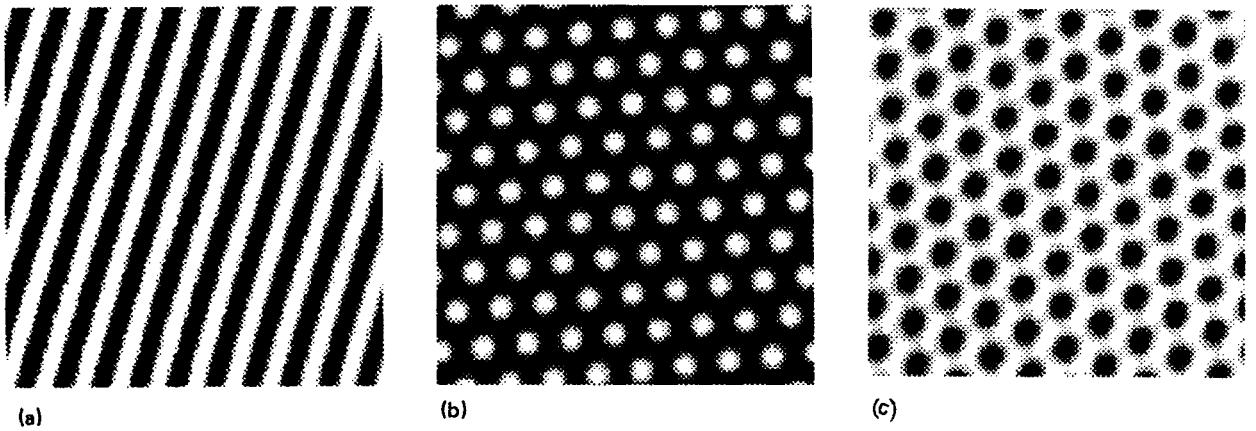

FIG. 2. Striped and hexagonal patterns. (a) striped pattern ($a = 0.14$, $b = 1.41$, size: 1.1×1.14, grid: 110×114); (b) hexagonal pattern type H2 ($a = 0.21$, $b = 1.1222$, size: 1.1×1.14, grid: 110×114); (c) hexagonal pattern type H1 ($a = 0.14$, $b = 1.421$, size: 1.06×1.06, grid: 106×106).

mains is surprisingly sharp. Rhombs were never observed *with these initial conditions.*

B. Bifurcation analysis

In order to characterize the bifurcation, we studied very finely the nature of the patterns and the amplitude of the spatial oscillations of the variable u as a function of $\delta b = b_c - b$ for $a = 0.14$.

We start far from the bifurcation point, inside the Turing space, with a stable hexagonal structure of type H2. When decreasing $b_c - b$, the hexagonal structure becomes unstable, and the system jumps to a striped pattern (Fig. 3). The reverse transition occurs with hysteresis when b is decreased. The striped organization persists up to the vicinity of the bifurcation point with strongly decreasing amplitude. In order to avoid spurious effects due to mode quantification (Ref. 1, p. 113), we have carefully studied the amplitude and stability of stripes with $k = k_c$ in this region (Fig. 4). Very close to the bifurcation point the striped pattern becomes unstable [Fig. 4(a)]. Instead of the stripes, a stable hexagonal pattern of type H1 is observed in a tiny region around the bifurcation point. The bifurcation from the uniform state to this hexagon's branch is subcritical, with a finite amplitude as shown in Fig. 4(b), but the hysteresis range is extremely small ($\delta b / b \sim 2 \times 10^{-4}$). Except for this region, the

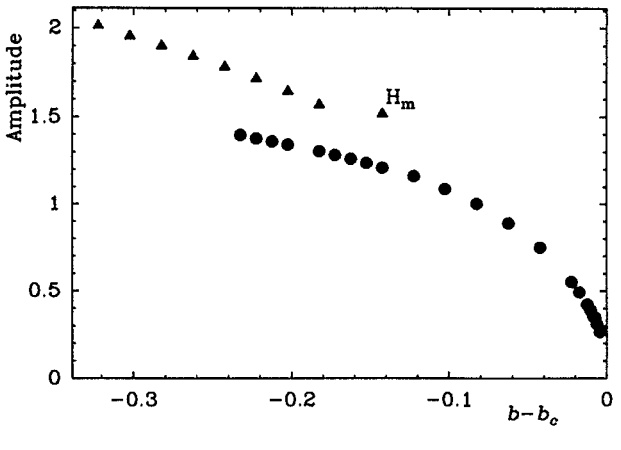

FIG. 3. Bifurcation diagram: amplitude of u pattern vs $(b - b_c)$. $a = 0.14$, $b_c = 1.4224$, size: 1.10×1.14 (grid:100×114) ▲: stable hexagons; ●: stable parallel or undulated stripes; for point H_m see Fig. 11 (Sec. IV D).

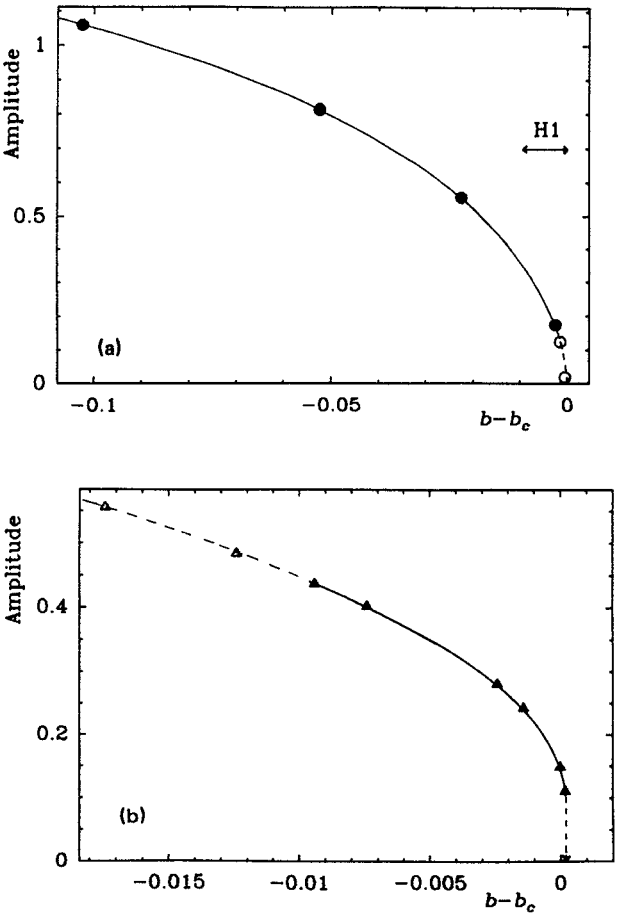

FIG. 4. Bifurcation diagram (mode $k \simeq k_c$): amplitude of u vs $(b - b_c)$. $a = 0.14$, $b_c = 1.4224$, size: 1.06×1.06 (grid:106×106). (a) Striped pattern (●: stable stripes; ○: unstable stripes). The domain where the H1 hexagons are stable [see (b)] is reported. (b) Hexagonal pattern H1 (▲: H1 stable; △: H1 unstable).

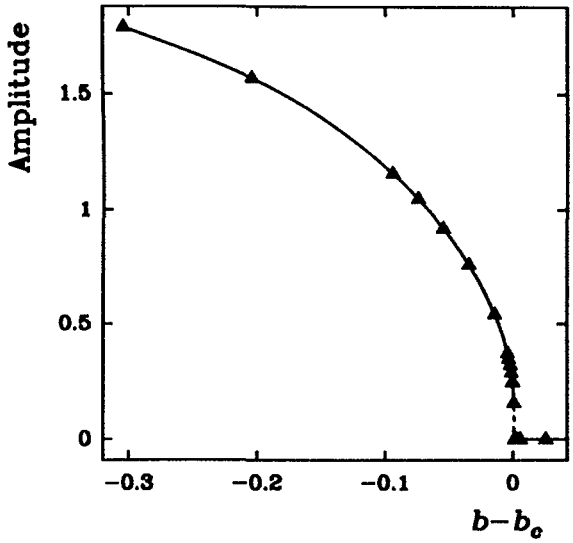

FIG. 5. Bifurcation diagram: amplitude of u pattern vs $(b - b_c)$. $a = 0.20$, $b_c = 1.1704$, size: 1.10×1.14 (grid: 100×114).

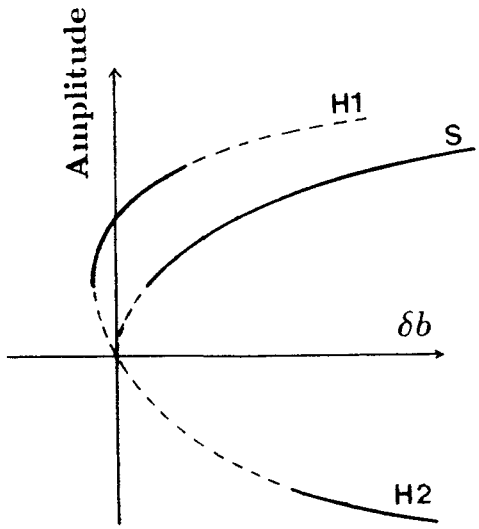

FIG. 6. Schematic bifurcation diagram at $a = 0.14$.—: stable states; - - -: unstable states.

striped pattern remains stable far from the bifurcation point [Fig. 4(a)]. The unstable states (computed in one dimension) indicate the supercritical character of this branch.

In another series of experiments, with $a = 0.20$, we have followed the transition from a uniform state to an hexagonal pattern (Fig. 5). Surprisingly, only hexagons of type H2 have been observed. Within the limitations of our numerical experiments, no other type of state has been evidenced close to the critical point. The bifurcation is subcritical as expected for an hexagonal branch, but the subcritical range is again extremely small ($\delta b / b \sim 10^{-3}$); the amplitude remains finite but decreases to values near zero.

C. Discussion

The results of the detailed study for $a = 0.14$ are in agreement with the theoretical schemes, if we assume that the quadratic term in the amplitude equations is small. The bifurcation scheme is represented in Fig. 6. To make these results easily understandable, the figure is not at scale and the bifurcation direction is reversed as usual. The first state has hexagonal symmetry (H1) and appears through a subcritical bifurcation, but since the quadratic term is small, the domain of hysteresis with the uniform state is very small, and the branch loses its stability close beyond the critical point (the stability domain strictly vanishes when the quadratic term is zero). The unstable supercritical branch of stripes recovers stability close to the critical point (the branch is stable at this point when the quadratic term is zero). Far from the bifurcation point the hexagon branch H2 also regains stability and prevails at large values of the bifurcation parameter. This is in agreement with recent computations and analytical calculations of the Brussels group on the Brussellator [Borkmans and Dewel (private communications)].

The behavior at $a = 0.20$ is less clear. Again, the first arising pattern is hexagonal, but with type H2, which seems to indicate a change of sign for a value $0.14 < a < 0.20$. Although the subcritical domain is slightly wider than in the case $a = 0.14$, it is yet very small. It is thus surprising that the branch does not lose its stability when the distance from the bifurcation point increases. A possible explanation is the shape of the Turing space limit which present a turning point (horizontal tangent) for $a \simeq 0.24$. This maintains the system in the vicinity of the bifurcation even at large values of $|\delta b|$.

According to the theory of pattern formation, beyond the bifurcation point, an increasing number of modes can become unstable. Nevertheless, only a limited range of the corresponding wave vectors can be selected. The other growing modes are destabilized through nonlinear coupling. In the context of fluid mechanics, the secondary instabilities of striped patterns have been investigated starting from the relevant amplitude equation, the Newell–Whitehead–Segel equation.[36] (For a review, see Ref. 15.) We shall now systematically consider these generic instabilities and show that they actually occur in our system, leading eventually to regular stripes, but also to less conventional systems of stripes, the zigzag patterns. We have seen, that except for a tiny region, just beyond the bifurcation point, we have observed stable stripes for $a = 0.14$. Neglecting the effects of the small quadratic term, we return to these patterns for our present study.

IV. STRIPES INSTABILITIES AND ZIGZAG PATTERNS

A. Stability diagram

For $a = 0.14$, the critical parameters are: $b_c = 1.42\,241...$, $k_c = 59.1072...$. Just beyond the bifurcation point, the real part of the eigenvalue associated with the unstable mode is[15]

$$\tau\sigma = \delta b - \xi_0^2 \delta k^2, \tag{4}$$

where $\delta b = b_c - b$, $\delta k = k - k_c$, τ is a typical characteristic time, and ξ_0 is the coherence length. Developing the eigen-

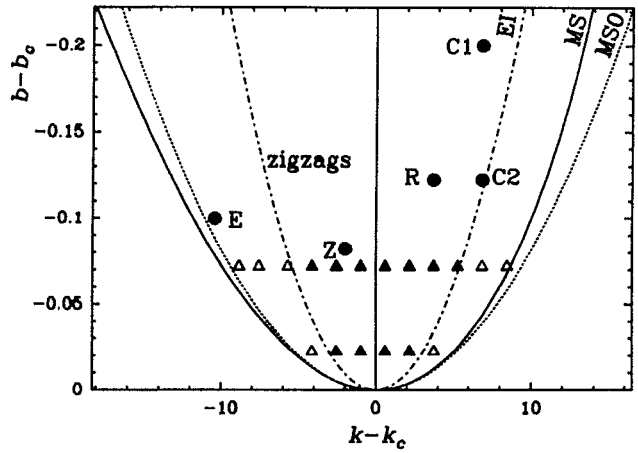

FIG. 7. Stability diagram. $a = 0.14$, $b_c = 1.4224$, $k_c = 59.107$; MS: exact marginal stability curve; MSO: marginal stability curve from Eq. (5); EI: Eckhaus stability limits △: Eckhaus unstable modes; ▲: Eckhaus stable modes. Points R,C1,C2,E,Z define conditions for experiments in Secs. IV B to IV D.

value of the Schnackenberg model with help of a symbolic analyzer, we found the following values for the considered bifurcation: $\tau = 2.62\times10^{-4}$, $\xi_0 = 0.028$,..., and on the marginal stability curve $\sigma = 0$,

$$\delta b = 8.184\times10^{-4}\delta k^2. \tag{5}$$

This parabola and the exact stability curve are represented on Fig. 7. They will be used further to locate different experimental points and stability domains.

B. "Cross rolls" and similar instabilities

This "amplitude" instability corresponds to large wave numbers and develops over a short time scale. Since for a given b, the oscillation amplitudes are larger for modes with $k\sim k_c$ than for marginal modes, the system tends to destroy the latter in order to develop the former. We start from a striped pattern with a linearly unstable but far from k_c wave number. We add a small amplitude perturbation (not visible on the figures), made of a system of stripes with $k\sim k_c$ at a different orientation. The perturbation grows and imposes its own wavelength and orientation (or a close one) to the eventual pattern. Two examples, respectively those of a "cross roll" and of an "oblique roll" instability are given in Fig. 8.

At smaller values of b, and with the same type of perturbation, we have also observed a surprising transition to a stable rhombic pattern. [Fig 9(a)]. The angle of the diamond formed by the two basic wave vectors is 50 degrees. [Fig. 9(b)]. This is the only example of a rhombic pattern obtained in our simulations.

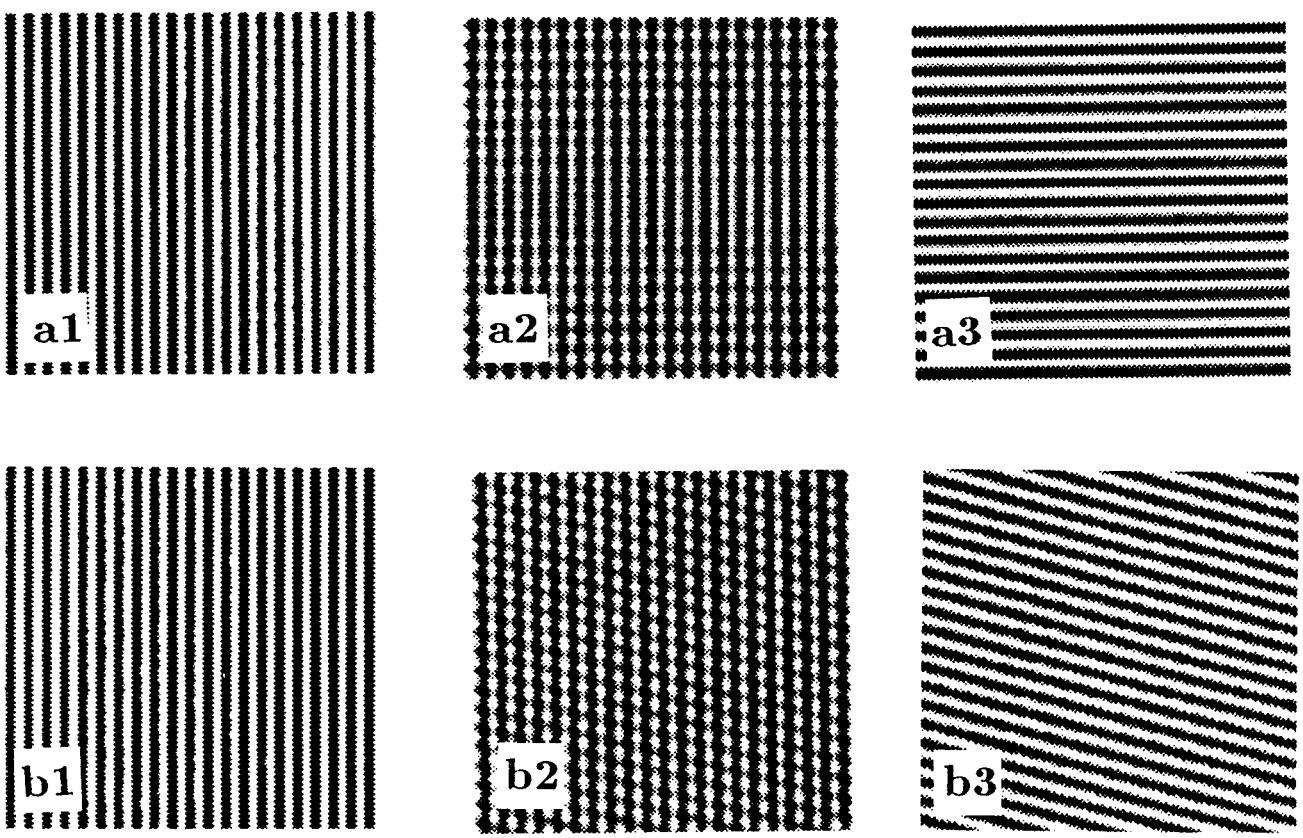

FIG. 8. Amplitude instabilities. Size: 2×2 (grid: 200×200). (a) "Cross-roll" instability (point C1 on Fig. 7). $a = 0.14$, $b = 1.2224$ $a1$: initial pattern (vertical stripes with small amplitude horizontal stripes added); $a2$: transient pattern obtained at time $t = 0.01$; $a3$: final pattern ($t = 0.0668$). (b) "oblique-roll" instability (point C2 on Fig. 7). $a = 0.14$, $b = 1.3$ $b1$: initial pattern stripes with small amplitude oblique stripes added; $b2$: transient pattern ($t = 0.02$); $b3$: final pattern ($t = 0.118$).

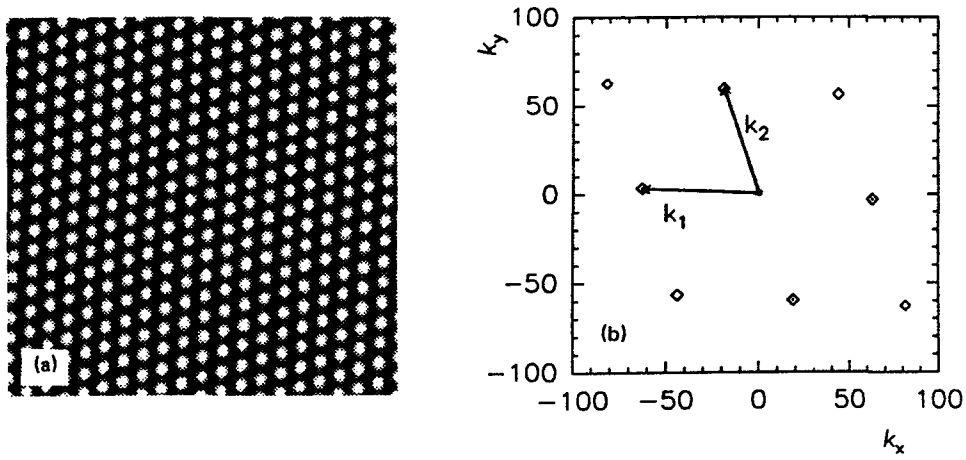

FIG. 9. Rhombic pattern. (a) Final pattern (point R in Fig. 7). Initial pattern: vertical stripes with small amplitude oblique stripes added; $a = 0.14$, $b = 1.3$; size: 2×2 (grid: 200×200); (b) Fourier transform of the pattern; main peaks and secondary peaks with relative amplitude larger than 1%.

C. Eckhaus instability

The Eckhaus instability is a slow phase instability arising in the direction of the wave vector. This instability results from the symmetry breaking of translational invariance and governs the selection process in one-dimensional systems.[37,38] The unstable modes are (at lowest order) located between the marginal stability curve $\delta b = \xi_0^2 \delta k^2$ and the curve $\delta b = 3\xi_0^2 \delta k^2$ (Fig. 7). We neglect here, the small universal corrections due to the quantification of modes, recently calculated by Tuckerman and Barkley.[39] The creation or annihilation of stripes[38,39] necessary to adjust the wave number corresponds to local compressions and dilatations of the pattern. We have checked the stability of all permitted modes of our model at several values of δb in 1D computations. The results reported in Fig. 7 are in excellent agreement with the predictions. A two-dimensional example is given in Fig. 10. We have chosen a narrow box to avoid the development of long range transverse parasitic instabilities.

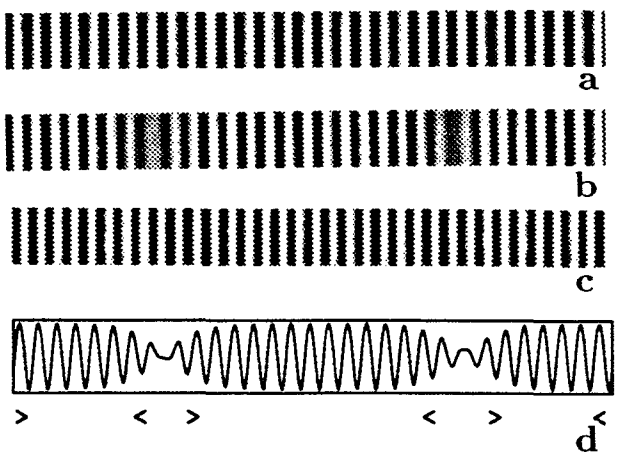

FIG. 10. Eckhaus instability (point E on Fig. 7). (a) Initial state: vertical stripes with small amplitude and large wave vector modulation added; (b) transient pattern ($t = 0.0408$); (c) final pattern ($t = 0.0902$); (d) spatial profile of pattern 10(b). $a = 0.14$, $b = 1.3224$; size: $4. \times 0.4$ (grid 400×40).

D. Zigzag instability and zigzag patterns

The zigzag instability is a phase instability induced by perturbations transverse to the wave vector. It is associated with the symmetry breaking of rotational invariance. The instability occurs (at lowest order) for all modes with $\delta k < 0$ and takes the form of a large undulation of stripes. The effect is to decrease the mean wavelength favoring modes with $k \sim k_c$ (at higher orders, slightly negative δk are also allowed), but, since it generates transverse modes, the final pattern may exhibit different orientations or symmetry. In Fig. 11, we present two examples of a zigzag instability, leading respectively to a different system of stripes and to a system of hexagons.

Actually, the most remarkable property of the zigzag instability is its capability to saturate without further change of orientation or change of symmetry. Thus, stable zigzag patterns are indeed observed in large domains of parameters. In Fig. 12, zigzags arise from the destabilization of the parallel stripes by a small perturbation made of oblique stripes, with a wavelength large with respect to the critical wavelength (phase modulation). Note the difference from the oblique roll instability, where the perturbation wave vector belongs to the range of linearly unstable modes. In the bifurcation diagram of Fig. 3, we did not distinguish between parallel and undulated patterns but a number of the striped pattern were of zigzag type. At the transition from the hexagonal branch, the resulting stripes were truly zigzags, not parallel stripes. This structure persisted in the range $1.28 < b < 1.40$. These zigzag patterns are somewhat unconventional since they share features both of one-dimensional and two-dimensional structures. Actually, as shown in Fig. 11, when the instability is not "self-saturated," they are just transients in the formation of stripes (1D case) or of hexagons (2D case). Moreover, we commonly obtained zigzag patterns, starting from uniform conditions with random noise. They do not develop only from a specific perturbation.

The zigzag patterns also arise spontaneously in textures that form in weakly confined systems from a uniform state. In Fig. 13, we present the spontaneous emergence of structures in a weakly confined system, i.e., a system large enough

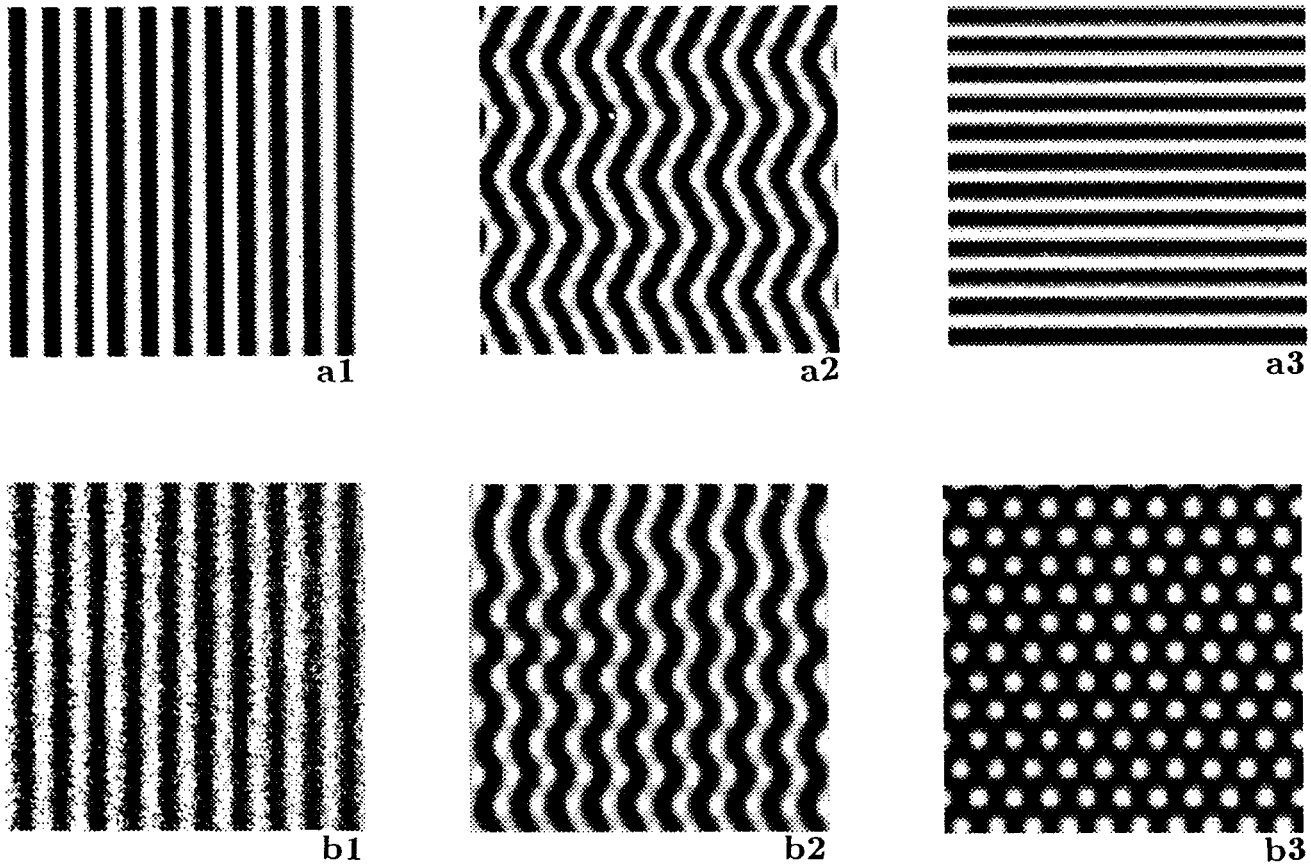

FIG. 11. Zigzag instability. (a) Transition from unstable striped state to stable striped pattern. $a = 0.14$, $b = 1.32$; size: 1.28×1.28 (grid 128×128); $a1$: initial pattern: stripes with small amplitude oblique stripes added; $a2$: transient pattern ($t = 0.2$); $a3$: final pattern ($t = 0.6363$). (b) Transition from unstable striped pattern to a hexagonal pattern. The final pattern corresponds to point H_m in Fig. 3 (the discontinuity with the other branch H2 results from a small change of wavelength). $a = 0.14$, $b = 1.28$; size: 1.20×1.20 (grid 120×120); $b1$: initial striped pattern with random noise added; $b2$: transient pattern ($t = 0.037$); $b3$: final pattern ($t = 0.2284$).

to cause the structure to nucleate at various locations. Starting from a uniform state with random noise, the concentrations slowly evolve to form a system of well organized domains, separated by lines of defects. In this example, the stripes are not parallel, but clearly form local zigzag patterns.

For information, we also report (Fig. 14) the temporal evolution of a weakly confined system when the parameters

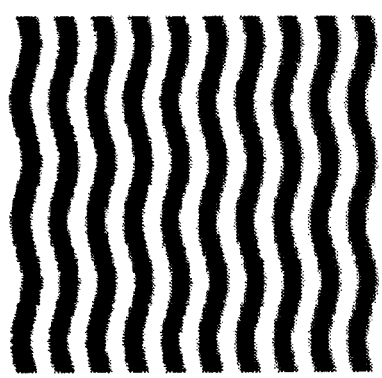

FIG. 12. Zigzag pattern (point Z on Fig. 7). Initial state: vertical stripes with small oblique amplitude stripes added $a = 0.14$, $b = 1.34$, size: 2×2 (grid: 200×200).

correspond to prevailing hexagonal symmetry. They are in good qualitative agreement with the experimental patterns of Ref. 13.

V. CONCLUSION

We have systematically compared the 2D Turing structures obtained in direct simulations of the dynamics of a typical model reaction–diffusion scheme with the general theoretical predictions.

We observe conventional striped and hexagonal patterns, with large domains of bistability. Nevertheless, the striped patterns appear to be more general than expected for systems without particular symmetry. Moreover, the bifurcation to hexagonal branches is only slightly subcritical; thus, the system behaves as if the quadratic term were small. Similar behavior were observed with the Brussellator as shown in Refs. 21 and 22 and could be a common situation in chemical systems. In practice, it is difficult to distinguish such a subcritical discontinuous transition from a continuous one, which very likely explains the experimental observations of Ref. 13 where the authors report a quasicontinuous transition from a uniform to an hexagonal state. Their experimental results can be compared with our bifurcation diagram of the Fig. 5. Like in our numerical studies, hexag-

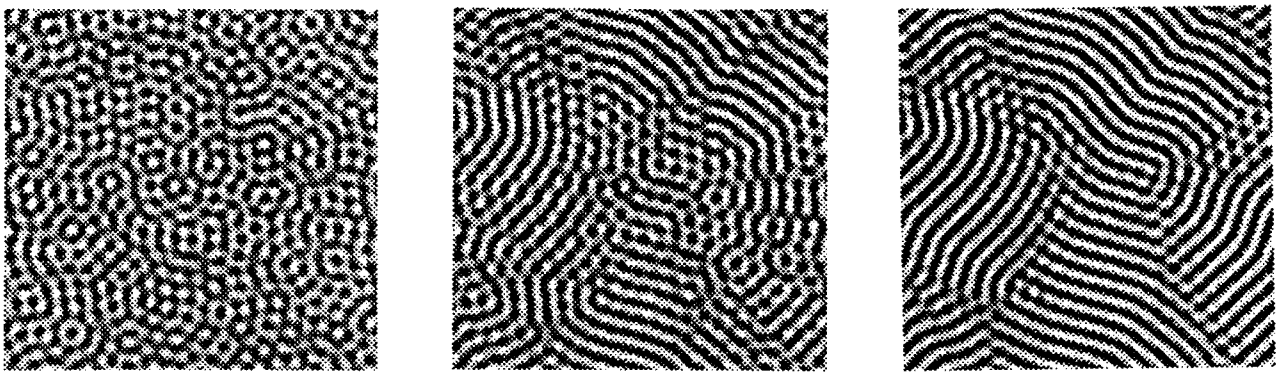

FIG. 13. Formation of zigzag domains in a weakly confined system. $a = 0.14$, $b = 1.4$, size: 2.5×2.5 (grid: 250×250). Initial pattern was uniform state with random noise added. Different stages of the evolution (a: $t = 0.05$; b: $t = 0.15$; c: $t = 0.35$).

onal symmetry generally prevails but large regions of stripe patterns are also observed. In our simulations, the last type of regular patterns, rhombic patterns, has only been observed once, for parameters which also lead to stable stripes.

All the generic instabilities of striped pattern predicted in hydrodynamics, and experimentally observed, are well reproduced with the chemical scheme: "cross rolls" or "oblique rolls," Eckhaus and zigzag instabilities. The zigzag instability leads to ubiquitous stable zigzag patterns, including within weakly confined systems. The exact nature of patterns is important in biological applications and many efforts have been devoted to their precise design. Thus, the zigzag patterns, which introduce an additional intrinsic wavelength, must be distinguished from regular stripes. As we have shown, they share some features of higher dimensionality structures. In three dimensional systems, one expects additional complexity when the planes (i.e., stripes in three dimensions) are destabilized by a zigzag instability. The resulting substructure in the planes is presently under investigation.

To conclude, we want to emphasize the interest of chemical systems for the study of nonlinear patterns. The recent experimental success in the search for Turing patterns opens new perspectives in this field.

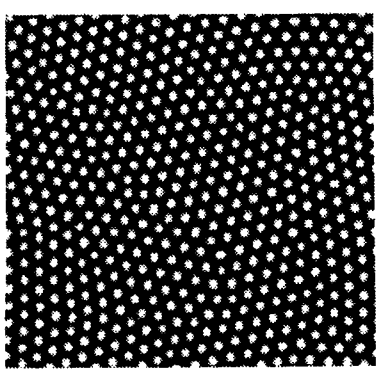

FIG. 14. Hexagonal domains in a weakly confined system. $a = 0.14$, $b = 1.14$, size: 2.5×2.5 (grid: 250×250). Initial pattern was uniform state with random noise added.

ACKNOWLEDGMENTS

We are indebted to A. Arneodo, E. Dulos, and P. De Kepper for daily stimulating and enlightning discussions and to A. De Wit, P. Borckmans, G. Dewel, Q. Ouyang, and H. Swinney for numerous technical informations and criticism of the manuscript. This work has been supported by the Venture Research Unit of British Petroleum.

[1] G. Nicolis and I. Prigogine, *Self-organization in Nonequilibrium Chemical Systems* (Wiley, New York, 1977).
[2] H. Haken, *Synergetics, an Introduction* (Springer-Verlag, Berlin, 1977).
[3] *Oscillations and Traveling Waves in Chemical Systems*, edited by R. J. Field and M. Burger (Wiley, New York, 1985).
[4] J. D. Murray, *Mathematical Biology* (Springer-Verlag, Berlin, 1989).
[5] P. Gray and S. Scott, *Chemical Oscillations and Instabilities* (Clarendon, Oxford, 1990).
[6] A. M. Turing, Philos. Trans. R. Soc. London, Ser. B **327**, 37 (1952).
[7] H. Meinhardt, *Models of Biological Patterns Formation* (Academic, New York, 1982).
[8] A. Babloyantz, *Molecules, Dynamics, and Life* (Wiley, New York, 1986).
[9] L. G. Harrison, J. Theor. Biol. **185**, 369 (1987).
[10] V. Castets, E. Dulos, J. Boissonade, and P. De Kepper, Phys. Rev. Lett. **64**, 2953 (1990).
[11] P. De Kepper, V. Castets, E. Dulos, and J. Boissonade, Physica D **49**, 161 (1991).
[12] J. Boissonade, V. Castets, E. Dulos, and P. De Kepper, ISNM **97** (Birkhäuser, Basel, 1991), pp. 67–77.
[13] Q. Ouyang and H. L. Swinney, Nature **352**, 610 (1991).
[14] I. Lengyel and I. R. Epstein, Science **251**, 650 (1990).
[15] P. Manneville, *Dissipative Structures and Weak Turbulence* (Academic, New York, 1990).
[16] H. Haken and H. Olbrich, J. Math. Biol. **6**, 317 (1978).
[17] L. M. Pismen, J. Chem. Phys. **72**, 1900 (1980).
[18] D. Walgraef, G. Dewel, and P. Borckmans, Phys. Rev. A **21**, 397 (1980).
[19] Y. Kuramoto, *Chemical Oscillations, Waves, and Turbulence* (Springer, Berlin, 1984).
[20] D. Walgraef, G. Dewel, and P. Borckmans, Adv. Chem. Phys. **49**, 311 (1982); D. Walgraef, *Structures spatiales loin de l'équilibre* (Masson, Paris, 1988).
[21] A. De Wit, G. Dewel, and P. Borckmans, in *Seeds: Genesis of Natural and Artificial Forms*, edited by Le Biopole Végétal (Amiens, France, 1990), p. 62.
[22] A. De Wit, G. Dewel, P. Borckmans, and D. Walgraef, Physica D (in press).
[23] M. J. Lyons and L. G. Harrison, Chem. Phys. Lett. **183**, 158 (1991).
[24] J. Schnackenberg, J. Theor. Biol. **81**, 389 (1979).
[25] I. Prigogine and R. Lefever, J. Chem. Phys. **48**, 1695 (1968).
[26] J. D. Murray, J. Theor. Biol. **98**, 143 (1982).

[27] H. Fuji, M. Mimura, and Y. Nishiura, Physica D **5**, 1 (1982).
[28] P. Kaps and P. Rentrop, Numer. Math. **33**, 55 (1979).
[29] A. R. Gourlay, J. Inst. Math. Its Appl. **6**, 375 (1970).
[30] A. R. Gourlay and G. R. McGuire, J. Inst. Math. Its Appl. **7**, 216 (1971).
[31] L. Lapidus and G. Pinder, *Solutions of Spatial Differential Equations in Science and Engeenering* (Wiley, New York, 1982).
[32] T. C. Lacalli, Philos. Trans. R. Soc. London, Ser. B **294**, 547 (1981); T. C. Lacalli, D. A. Wilkinson, and L. G. Harrison, Development **104**, 105 (1988).
[33] F. H. Busse, J. Fluid Mech. **30**, 625 (1967).
[34] B. A. Malomed and M. I. Tribel'skii, Sov. Phys. JETP **65**, 305 (1987).
[35] S. Ciliberto, P. Coullet, J. Lega, E. Pampaloni, and C. Perez-Garcia, Phys. Rev. Lett. **65**, 2370 (1990).
[36] A. C. Newell and J. A. Whitehead, J. Fluid. Mech. **38**, 279 (1969); L. A. Segel, J. Fluid. Mech. **38**, 203 (1969).
[37] W. Eckhaus, *Studies in Nonlinear Stability Theory* (Springer, New York, 1965); J. T. Stuart and R. C. Di Prima, Proc. R. Soc. London, Ser. A **362**, 27 (1978).
[38] L. Kramer and W. Zimmermann, Physica D **16**, 221 (1985).
[39] L. Tuckerman and D. Barkley, Physica D **46**, 57 (1990).